Inorganic Chemistry

Article

pubs.acs.org/IC

Formation of a Metal-to-Nitrogen Bond of Normal Length by a Neutral Sufonamide Group within a Tridentate Ligand. A New Approach to Radiopharmaceutical Bioconjugation

Theshini Perera, Pramuditha Abhayawardhana, Patricia A. Marzilli, Frank R. Fronczek, and Luigi G. Marzilli*

Department of Chemistry, Louisiana State University, Baton Rouge, Louisiana 70803, United States

Supporting Information

ABSTRACT: We demonstrate that a tertiary sulfonamide group, $N(SO_2R)R'_2$, can rehybridize to form a M−N bond of normal length even when the group is in a linear tridentate ligand, such as in the new tridentate $N(SO_2R)$dpa ligands derived from di-(2-picolyl)amine (N(H)dpa). $N(SO_2R)$dpa ligands were used to prepare *fac*-[Re(CO)$_3$($N(SO_2R)$dpa)](PF$_6$ or BF$_4$) complexes. Structural characterization of the new complexes established that the tertiary sulfonamide nitrogen atom binds to Re with concomitant sp^2-to-sp^3 rehybridization, facilitating facial coordination. The new *fac*-[Re(CO)$_3$($N(SO_2R)$dpa)]X structures provide the only examples for any metal with the sulfonamide as part of a noncyclic linear tridentate ligand and with a normal metal-to-nitrogen(tertiary sulfonamide) bond length. Rare previous examples of such normal M−N bonds have been found only in more constrained situations, such as with tripodal tetradentate ligands. Our long-term objectives for the new tridentate $N(SO_2R)$dpa ligands are to develop the fundamental chemistry relevant to the eventual use of the *fac*-[M^I(CO)$_3$]$^+$ core (M = ^{99m}Tc, $^{186/188}$Re) in imaging and therapy. The sulfonamide group uniquely contributes to two of our goals: expanding ways to conjugate the *fac*-[M^I(CO)$_3$]$^+$ core to biological molecules and also developing new symmetrical tridentate ligands that can coordinate facially to this core. Tests of our conjugation method, conducted by linking the *fac*-[Re^I(CO)$_3$]$^+$ core to a new tetraarylporphyrin (T($N(SO_2C_6H_4)$dpa)P) as well as to a dansyl (5-(dimethylamino)naphthalene-1-sulfonyl) group, demonstrate that large molecular fragments can be tethered via a coordinated tertiary sulfonamide linkage to this core.

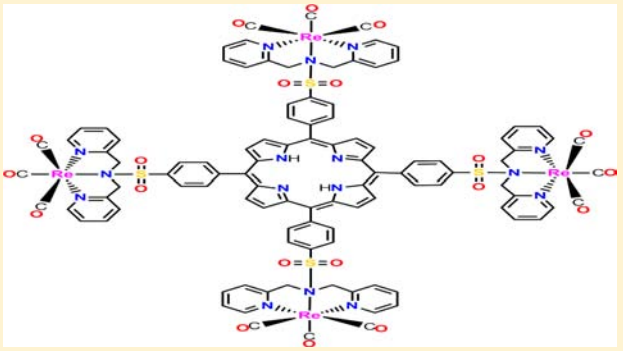

INTRODUCTION

Improved methods of ligand design are needed for the synthesis of radiopharmaceuticals containing the *fac*-[^{99m}Tc^I(CO)$_3$]$^+$ core; such agents have received widespread attention in the past two decades.[1−6] Many factors have contributed to this interest, including the convenient generation of the *fac*-[^{99m}Tc(CO)$_3$(H$_2$O)$_3$]$^+$ precursor,[7,8] the stability and kinetic inertness of *fac*-[^{99m}Tc(CO)$_3$L]^n imaging agents when L is a facially coordinated tridentate ligand,[1,4,9] and the potential that novel ligands bound to this core will lead to agents with new or superior clinical utility.[10] Such *fac*-[^{99m}Tc(CO)$_3$L]^n agents have been shown to possess desirable biological characteristics in human volunteers,[4,11] with *fac*-[^{99m}Tc(CO)$_3$(NTA)]$^{2-}$ (NTA = nitrilotriacetate)[11] showing promise as a renal imaging agent in early patient studies.[12] Historically, the study of nonradioactive Re analogues has played an important role in guiding ligand design and in providing a basis for understanding the chemistry of ^{99m}Tc diagnostic agents and $^{186/188}$Re therapeutic agents.[1,13,14] Likewise, many *fac*-[Re(CO)$_3$L]^n analogues have more recently facilitated the *fac*-[^{99m}Tc(CO)$_3$L]^n biomedical studies by serving as models that allow insight into the chemistry and biomedical characteristics of these short-lived radioactive ^{99m}Tc imaging agents.[4,15−20]

Symmetrical linear tridentate ligands that do not induce asymmetry at the metal center are desirable for avoiding racemic or diastereoisomeric mixtures of radiopharmaceuticals. For example, di-(2-picolyl)amine (N(H)dpa) forms a symmetrical complex, *fac*-[Re(CO)$_3$(N(H)dpa)]X.[21] Promising biomedical properties have been reported for *fac*-[Re(CO)$_3$(N(R)dpa)]^n complexes bearing a substituent linked by a C−N bond at the central sp^3 N, replacing the amine proton of N(H)dpa.[10,22,23] In referring to such ligands in this article, we use N(substituent)dpa, with the italic N designating the central nitrogen. Ligand design requires that the central donor of the tridentate ligand, such as the central sp^3 N in N(H)dpa or N(R)dpa, accommodates facial coordination. A thioether sulfur atom achieves this geometry,[16,24,25] but substituents imparting

Received: October 6, 2012
Published: February 19, 2013

 © 2013 American Chemical Society dx.doi.org/10.1021/ic302180t | Inorg. Chem. 2013, 52, 2412−2421

desirable biodistribution or targeting characteristics cannot be attached at a central sulfur donor atom.

Full exploitation of the *fac*-$[M^{I}(CO)_3]^+$ (M = ^{99m}Tc, Re) core relies on new types of tridentate ligands and ligand conjugation methods.[8,21,23] In this study, we explore conjugation utilizing an N−S bond by preparing new $N(SO_2R)$dpa ligands (R = Me, tmb, dmb, and Me_2Nnap; see Figure 1 for

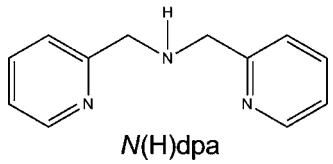

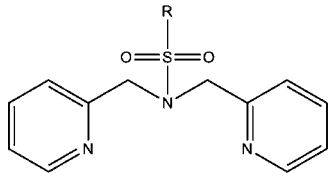

R = methyl
R = 2,4,6-trimethylbenzene
R = 3,5-dimethylbenzene
R = 4-methylbenzene
R = 5-(dimethylamino)naphthalene

Figure 1. Ligands mentioned or used in this study: di(2-picolyl)amine (N(H)dpa); *N,N*-di(2-picolyl)methanesulfonamide ($N(SO_2Me)$dpa); *N,N*-di(2-picolyl)-2,4,6-trimethylbenzenesulfonamide ($N(SO_2$tmb)dpa); *N,N*-di(2-picolyl)-3,5-dimethylbenzenesulfonamide ($N(SO_2$dmb)dpa); *N,N*-di(2-picolyl)-4-methylbenzenesulfonamide ($N(SO_2$tol)dpa); and *N,N*-di(2-picolyl)-5-(dimethylamino)-naphthalene-1-sulfonamide ($N(SO_2Me_2$Nnap)dpa).

ligand sketches and abbreviations). We show that treatment of *fac*-$[Re(CO)_3(H_2O)_3]^+$ with such open-chain tridentate $N(SO_2R)$dpa ligands affords *fac*-$[Re(CO)_3(N(SO_2R)dpa)]X$ complexes (Scheme 1), although the central *N*-donor atom is part of a tertiary sulfonamide group ($N(SO_2R)R'_2$). X-ray structural characterization shows that this nitrogen atom is a strong donor to Re. Our study of *fac*-$[Re(CO)_3(N(SO_2R)$-dpa)]X complexes provides the only examples of structurally characterized complexes with a tertiary neutral sulfonamide donor bound to the *fac*-$[Re^{I}(CO)_3]^+$ core. Furthermore, these compounds are the only examples of metal complexes in which any such open-chain tertiary sulfonamide linear tridentate ligand possesses a M−N(sulfonamide) bond of normal length, regardless of the metal center. Indeed, these are among the very few crystallographically characterized complexes containing tertiary sulfonamide N donors with any metal.[26−33] In previously reported sulfonamide complexes, the bound sulfonamide is either constrained within a ring system or has elongated bonds.[26−33]

In the design of new ligands, the nature of the geometric constraints induced by the central donor atoms is an important factor. The ligand should be able to coordinate facially. As an example, the propensity of thioethers to enforce a facial coordination mode[34,35] was utilized in designing renal agents, including agents bearing lanthionine dipeptide ligands.[4,16,17,36] These NSN-donor dipeptides with amino acids linked via a thioether group were used to study small *fac*-$[^{99m}Tc(CO)_3L]^n$

Scheme 1. Synthesis of *fac*-$[Re(CO)_3(N(SO_2R)dpa)]^+$ Complexes

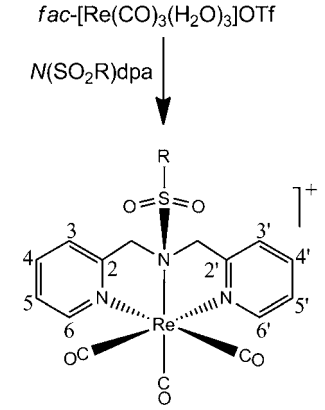

R = methyl	(**1**)
R = 2,4,6-trimethylbenzene	(**2**)
R = 3,5-dimethylbenzene	(**3**)
R = 4-methylbenzene	(**4**)
R = 5-(dimethylamino)naphthalene	(**5**)

agents in humans because the more traditional peptides coordinate with a deprotonated nitrogen, which enforces the meridional coordination mode.[4] The sulfonamide group explored here has an additional advantage over the thioether or peptide N-donor groups in being able to serve as a juncture point for conjugation. We validated the versatility of the sulfonamide method by conjugating the dansyl group or a tetraarylporphyrin biological targeting group to the *fac*-$[Re^{I}(CO)_3]^+$ core. (From this point on, we omit the *fac*-designation when discussing specific compounds because all compounds have this geometry.)

EXPERIMENTAL SECTION

Starting Materials. Methanesulfonyl chloride ($MeSO_2Cl$), 2,4,6-trimethylbenzenesulfonyl chloride ($tmbSO_2Cl$), 3,5-dimethylbenzenesulfonyl chloride ($dmbSO_2Cl$), 4-methylbenzenesulfonyl chloride ($tolSO_2Cl$), 5-(dimethylamino)naphthalene-1-sulfonyl chloride ($Me_2NnapSO_2Cl$, dansyl chloride), di-(2-picolyl)amine (N(H)dpa), and $Re_2(CO)_{10}$ were used as received from Aldrich. $[Re(CO)_3(H_2O)_3]$OTf (OTf = trifluoromethanesulfonate) was prepared by a known method.[36] $[Re(CO)_3(CH_3CN)_3]BF_4$ and *meso*-tetrakis(4-chlorosulfonylphenyl)porphyrin ($TClSO_2PP$) were synthesized as described elsewhere,[37,38] and their ^{1}H NMR spectra were in agreement with those reported.

NMR Measurements. ^{1}H NMR spectra were recorded on a Bruker 400 MHz spectrometer. Peak positions are relative to tetramethylsilane (TMS) or solvent residual peak with TMS as reference. All NMR data were processed with TopSpin and Mestre-C software.

X-ray Data Collection and Structure Determination. Intensity data were collected at low temperature on a Nonius Kappa CCD diffractometer fitted with an Oxford Cryostream cooler and graphite-monochromated Mo Kα (λ = 0.71073 Å) radiation. Data were collected at 90 K for **1** and **2**, but for **4** (T = 200 K) and **5** (T = 220 K), higher temperatures were chosen to avoid phase changes that occurred with twinning. Data reduction included absorption corrections by the multiscan method, using HKL SCALEPACK.[39] All X-ray structures were determined by direct methods and difference Fourier techniques and refined by full-matrix least-squares by using SHELXL97.[40] All non-hydrogen atoms were refined anisotropically. All H atoms except those on water molecules in **2** and **5** were visible in difference maps, but were placed in idealized positions. Those on

dx.doi.org/10.1021/ic302180t | Inorg. Chem. 2013, 52, 2412−2421

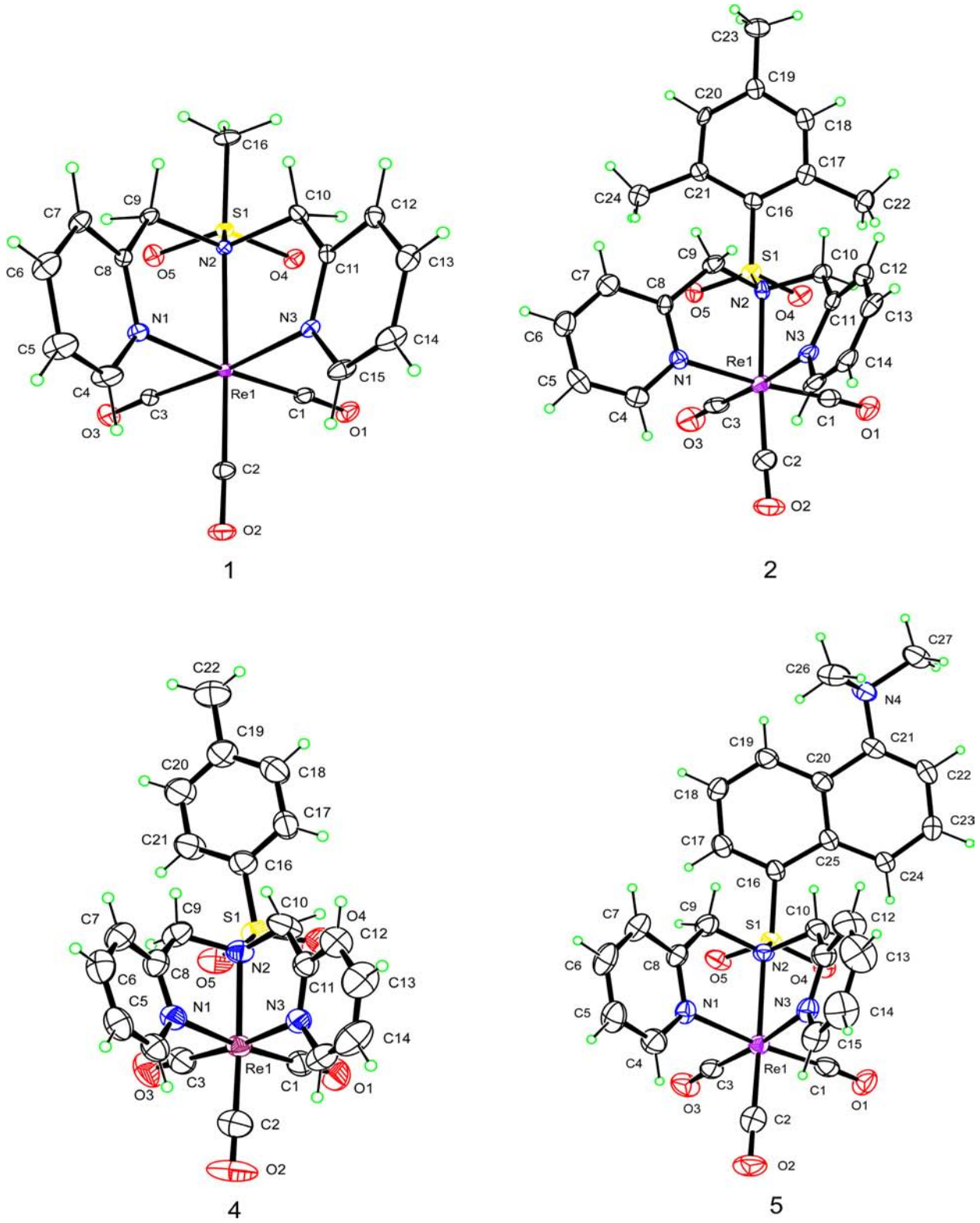

Figure 2. ORTEP plots of the cations in $[Re(CO)_3(N(SO_2Me)dpa)]PF_6$ (**1**), $[Re(CO)_3(N(SO_2tmb)dpa)]PF_6$ (**2**), $[Re(CO)_3(N(SO_2tol)dpa)]PF_6$ (**4**), and $[Re(CO)_3(N(SO_2Me_2Nnap)dpa)]BF_4$ (**5**). Thermal ellipsoids are drawn with 50% probability.

water were not located and are likely disordered. A torsional parameter was refined for each methyl group. For **1**, the PF_6^- anion was disordered into two positions treated with equal populations. For **5**, the BF_4^- anion site exhibited both substitutional and orientational disorder. The site was occupied by bromide with 6.8(3)% population, and the BF_4^- had two orientations with relative population 59(3):34(3)%. Structure **2** contains two independent formula units in the asymmetric unit, only one of which is shown in Figure 2. Crystal data and refinement details are included in Table 1.

Synthesis of $[Re(CO)_3L]PF_6$ and $[Re(CO)_3L]BF_4$ Complexes. The following general procedure was employed to obtain the $N(SO_2R)$dpa ligands: a solution of the sulfonyl chloride (0.9−1.5 g, 5 mmol) in 25 mL of dioxane was added dropwise over a period of 2 h to a solution of N(H)dpa (1.80 mL, 10 mmol) in 100 mL of dioxane

dx.doi.org/10.1021/ic302180t | Inorg. Chem. 2013, 52, 2412−2421

Table 1. Crystal Data and Structure Refinement for $[Re(CO)_3(N(SO_2Me)dpa)]PF_6$ (1), $[Re(CO)_3(N(SO_2tmb)dpa)]PF_6$ (2), $[Re(CO)_3(N(SO_2tol)dpa)]PF_6$ (4), and $[Re(CO)_3(N(SO_2Me_2Nnap)dpa)]BF_4$ (5)

	1[a]	2	4	5
empirical formula	$C_{16}H_{15}N_3O_5ReS{\cdot}PF_6$	$C_{24}H_{23}N_3O_5ReS{\cdot}PF_6{\cdot}H_2O$	$C_{22}H_{19}N_3O_5ReS{\cdot}PF_6$	$C_{27}H_{24}N_4O_5ReS{\cdot}0.93(BF_4){\cdot}0.07(Br){\cdot}4H_2O$
fw	692.54	814.70	768.63	861.58
crystal system	monoclinic	triclinic	monoclinic	monoclinic
space group	$C2/c$	$P\bar{1}$	$C2/c$	$C2/c$
unit cell dimensions				
a (Å)	20.549(2)	14.353(2)	15.102(2)	33.684(4)
b (Å)	20.297(2)	15.010(2)	10.4922(15)	8.1471(10)
c (Å)	12.5771(10)	16.028(3)	34.186(4)	23.635(3)
α (deg)	90	110.298(8)	90	90
β (deg)	123.039(4)	115.806(7)	100.598(4)	97.278(6)
γ (deg)	90	96.429(9)	90	90
V (Å^3)	4397.5(7)	2770.6(7)	5324.5(12)	6433.8(14)
T (K)	90	90	200	220
Z	8	4	8	8
ρ_{calc} (g/cm^3)	2.092	1.953	1.918	1.779
abs coeff (mm^{-1})	5.78	4.61	4.78	4.01
$2\theta_{max}$ (deg)	71.2	55.8	55.0	52.2
R[b] $[I > 2\sigma(I)]$	0.026	0.048	0.029	0.037
wR2[c]	0.055	0.105	0.087	0.088
res. dens (e Å^{-3})	−1.36, 1.58	−1.29, 1.41	−1.10, 1.20	−0.96, 1.09
data/param	10038/332	13140/764	5756/353	6317/456

[a]The asymmetric unit of **1** contains one $[Re(CO)_3(N(SO_2Me)dpa)]^+$ cation and half of two crystallographically independent PF_6^- anions; one anion lies on an inversion center, and the other anion lies on a 2-fold axis and is disordered. [b]$R = (\sum||F_o| - |F_c||)/\sum|F_o|$. [c]$wR2 = [\sum[w(F_o^2 - F_c^2)^2]/\sum[w(F_o^2)^2]]^{1/2}$, in which $w = 1/[\sigma^2(F_o^2) + (dP)^2 + (eP)]$ and $P = (F_o^2 + 2F_c^2)/3$; d = 0.021, 0.0463, 0.041, and 0.0399, and e = 0.6452, 0, 0, and 2.129 for **1**, **2**, **4**, and **5**, respectively.

at 20 °C. The reaction mixture was stirred at room temperature for 24 h and then filtered to remove any precipitate before the dioxane was completely removed by rotary evaporation. Water (30 mL, pH ∼5) was added to the resulting oil, and the product was extracted into CH_2Cl_2 (2 × 25 mL). The CH_2Cl_2 extracts were combined, washed with water (2 × 25 mL), and taken to dryness to yield an oil, which was used to synthesize $[Re(CO)_3L]PF_6$ and $[Re(CO)_3L]BF_4$ in the general procedure outlined here. The preparation utilized 0.1 mmol of the reactants. An aqueous solution of the ligand (0.1 mmol in 2 mL) was treated with aqueous $[Re(CO)_3(H_2O)_3]^+$ (0.1 mmol in 3 mL). Methanol (2−3 mL) was added to dissolve any precipitate that formed, and the clear reaction mixture was heated at reflux for 12 h. A slight excess of $NaPF_6$ or $NaBF_4$ was added to the clear solution, and the resulting precipitate was collected on a filter, washed with water, and air-dried. (If the pH of the final reaction mixture was below 6, it was adjusted to 7 before the addition of $NaPF_6$ or $NaBF_4$. For $N(SO_2tmb)dpa$ and $N(SO_2Me_2Nnap)dpa$, methanol (∼1 mL) was used initially to dissolve the ligand).

*$[Re(CO)_3(N(SO_2Me)dpa)]PF_6$ (**1**).* The general ligand preparative method described above, with $MeSO_2Cl$ (0.39 mL) and N(H)dpa (1.80 mL), yielded the crude $N(SO_2Me)dpa$ ligand as a deep red oil (1.40 g, 76% yield). ^{1}H NMR signals (ppm) in DMSO-d_6: 8.50 (d, J = 6.5 Hz, 2H, H6/6′), 7.75 (t, J = 7.6 Hz, 2H, H4/4′), 7.34 (d, J = 7.8 Hz, 2H, H3/3′), 7.27 (t, J = 6.5 Hz, 2H, H5/5′), 4.48 (s, 4H, CH_2), 3.11 (s, 3H, CH_3). In the 0.1 mmol preparative method described above, $N(SO_2Me)dpa$ (28 mg) was used. $[Re(CO)_3(N(SO_2Me)dpa)]PF_6$ formed as a white precipitate (38 mg, 54% yield) after the addition of $NaPF_6$ (∼15 mg). Slow evaporation of a solution of this compound in acetone produced colorless, needle-like crystals that were characterized crystallographically. ^{1}H NMR signals (ppm) in DMSO-d_6: 8.89 (d, J = 5.4 Hz, 2H, H6/6′), 8.09 (t, J = 6.7 Hz, 2H, H4/4′), 7.57 (d, 2H, H3/3′), 7.53 (t, J = 6.5 Hz, 2H, H5/5′), 5.44 (d, J = 15.8 Hz, 2H, CH_2), 5.13 (d, J = 15.8 Hz, 2H, CH_2), 3.87 (s, 3H, CH_3).

*$[Re(CO)_3(N(SO_2tmb)dpa)]PF_6$ (**2**).* The general method described above, with $tmbSO_2Cl$ (1.10 g) and N(H)dpa (1.80 mL), yielded $N(SO_2tmb)dpa$ as a pale orange oil (1.75 g, 92% yield). ^{1}H NMR signals (ppm) in DMSO-d_6: 8.43 (d, J = 6.4 Hz, 2H, H6/6′), 7.65 (t, J = 7.9 Hz, 2H, H4/4′), 7.22 (t, J = 6.1 Hz, 2H, H5/5′), 7.09 (d, J = 7.8 Hz, 2H, H3/3′), 6.97 (s, 2H, H3/5), 4.53 (s, 4H, CH_2), 2.53 (s, 6H, CH_3), 2.23 (s, 3H, CH_3). In the 0.1 mmol preparative method, $N(SO_2tmb)dpa$ (38 mg) afforded $[Re(CO)_3(N(SO_2tmb)dpa)]PF_6$ as a white precipitate (51 mg, 64% yield) after the addition of $NaPF_6$ (∼15 mg). Slow evaporation of a solution of the compound in $CHCl_3$ produced colorless, block-shaped crystals that were characterized crystallographically. ^{1}H NMR signals (ppm) in DMSO-d_6: 8.90 (d, J = 5.4 Hz, 2H, H6/6′), 8.05 (t, J = 7.8 Hz, 2H, H4/4′), 7.64 (d, J = 7.8 Hz, 2H, H3/3′), 7.49 (t, J = 6.6 Hz, 2H, H5/5′), 7.46 (s, 2H, H3/5), 5.22 (d, J = 15.9 Hz, 2H, CH_2), 4.53 (d, J = 15.9 Hz, 2H, CH_2), 2.78 (s, 6H, CH_3), 2.43 (s, 3H, CH_3).

*$[Re(CO)_3(N(SO_2dmb)dpa)]BF_4$ (**3**).* The general method described above, with $dmbSO_2Cl$ (1.02 g) and N(H)dpa (1.80 mL), yielded $N(SO_2dmb)dpa$ as a pale orange oil (1.45 g, 86% yield). ^{1}H NMR signals (ppm) in DMSO-d_6: 8.37 (d, J = 5.6 Hz, 2H, H6/6′), 7.67 (t, J = 6.8 Hz, 2H, H4/4′), 7.35 (s, 2H, H2/6), 7.28 (d, J = 7.8 Hz, 2H, H3/3′), 7.21 (s, 1H, H4), 7.19 (t, J = 5.9 Hz, 2H, H5/5′), 4.54 (s, 4H, CH_2), 2.29 (s, 6H, CH_3). In the 0.1 mmol preparative method, $N(SO_2dmb)dpa$ (37 mg) afforded $[Re(CO)_3(N(SO_2dmb)dpa)]BF_4$ as a white precipitate (55 mg, 67% yield) after the addition of $NaBF_4$ (∼15 mg). ^{1}H NMR signals (ppm) in DMSO-d_6: 8.88 (d, J = 5.4 Hz, 2H, H6/6′), 8.02 (t, J = 7.7 Hz, 2H, H4/4′), 7.96 (s, 2H, H2/6), 7.72 (s, 1H, H4), 7.51 (d, J = 8.4 Hz, 2H, H3/3′), 7.46 (t, J = 6.4 Hz, 2H, H5/5′), 5.25 (d, J = 16.2 Hz, 2H, CH_2), 4.55 (d, J = 16.2 Hz, 2H, CH_2), 2.51 (s, 6H, CH_3, overlap with solvent residual peak). Anal. Calcd for $C_{23}H_{21}BF_4N_3O_5ReS$: C, 38.10; H, 2.92; N, 5.80. Found: C, 37.87; H, 2.83; N, 5.88.

*$[Re(CO)_3(N(SO_2tol)dpa)]PF_6$ (**4**).* The general method described above, with $tolSO_2Cl$ (0.95 g) and N(H)dpa (1.80 mL), yielded $N(SO_2tol)dpa$ as a deep brown oil (1.52 g, 86% yield). ^{1}H NMR signals (ppm) in DMSO-d_6: 8.35 (d, J = 4.8 Hz, 2H, H6/6′), 7.70 (d, J = 8.2 Hz, 2H, H2/6), 7.65 (t, J = 7.7 Hz, 2H, H4/4′), 7.36 (d, J = 8.0 Hz, 2H, H3/5), 7.25 (d, J = 7.8 Hz, 2H, H3/3′), 7.19 (t, J = 4.9 Hz, 2H, H5/5′), 4.49 (s, 4H, CH_2), 2.39 (s, 3H, CH_3). In the 0.1 mmol preparative method, $N(SO_2tol)dpa$ (35 mg) afforded [Re-

dx.doi.org/10.1021/ic302180t | Inorg. Chem. 2013, 52, 2412−2421

Scheme 2. Synthesis of T(N($SO_2C_6H_4$)dpa)P

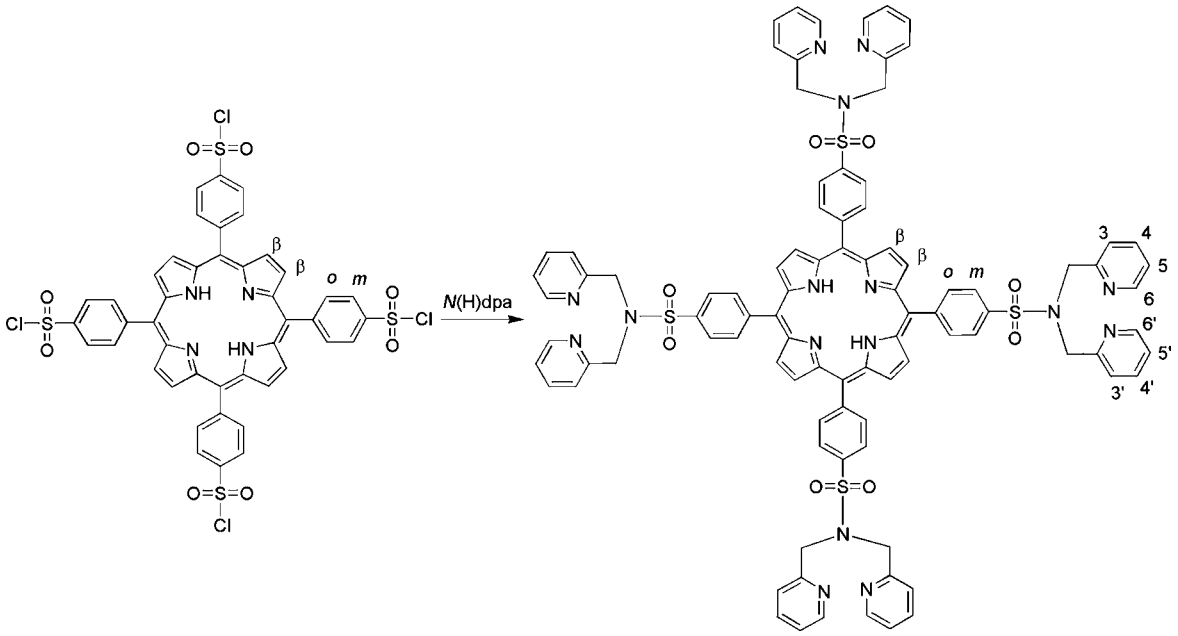

$(CO)_3(N(SO_2tmb)dpa)]PF_6$ as a white precipitate (50 mg, 65% yield) after the addition of $NaPF_6$ (~15 mg). Slow evaporation of a solution of the compound in $CHCl_3$ produced colorless, block-shaped crystals that were characterized crystallographically. ^{1}H NMR signals (ppm) in DMSO-d_6: 8.87 (d, J = 5.4 Hz, 2H, H6/6′), 8.21 (d, J = 8.4 Hz, 2H, H2/6), 8.02 (t, J = 7.8 Hz, 2H, H4/4′), 7.76 (d, J = 8.4 Hz, 2H, H3/5), 7.48 (d, J = 7.9 Hz, 2H, H3/3′), 7.47 (t, 2H, H5/5′), 5.58 (d, J = 16.0 Hz, 2H), 4.53 (d, J = 16.0 Hz, 2H), 2.57 (s, 3H, CH_3).

*[Re(CO)$_3$(N(SO$_2$Me$_2$Nnap)dpa)]BF$_4$ (**5**).* The general method described above, with dansyl chloride (1.42 g) and N(H)dpa (1.8 mL), yielded N(SO_2Me_2Nnap)dpa as a pale orange oil (1.96 g, 91% yield). ^{1}H NMR signals (ppm) in DMSO-d_6: 8.44 (d, J = 8.5 Hz, 1H), 8.37 (d, J = 4.5 Hz, 2H, H6/6′), 8.20 (d, J = 8.6 Hz, 1H), 8.16 (d, J = 7.3 Hz, 1H), 7.58 (t, 2H, H4/4′), 7.54 (m, 2H), 7.23 (d, J = 7.6 Hz, 1H), 7.18 (t, 2H, H5/5′), 7.12 (d, J = 7.8 Hz, 2H, H3/3′), 4.72 (s, 4H, CH_2), 2.82 (s, 6H, CH_3). In the 0.1 mmol preparative method, N(SO_2Me_2Nnap)dpa (43 mg) afforded [Re(CO)$_3$(N(SO_2Me_2Nnap)-dpa)]BF_4 as yellow block-like crystals (38 mg, 44% yield) after the addition of $NaBF_4$ (~15 mg). The product was characterized crystallographically. ^{1}H NMR signals (ppm) in DMSO-d_6: 8.90 (m, 3H), 8.71 (d, J = 7.7 Hz, 1H), 8.58 (d, J = 8.7 Hz, 1H), 7.98 (t, J = 8.1 Hz, 2H, H4/4′), 7.92 (t, J = 7.9 Hz, 1H), 7.78 (t, J = 8.2 Hz, 1H), 7.47 (t, J = 6.6 Hz, 2H, H5/5′), 7.42 (d, J = 7.6 Hz, 2H, H3/3′), 7.39 (d, J = 7.9 Hz, 1H), 5.64 (d, J = 15.7 Hz, 2H), 4.53 (d, J = 15.8 Hz, 2H, CH_2), 2.91 (s, 6H, CH_3).

T(N(SO$_2$C$_6$H$_4$)dpa)P. A solution of $TClSO_2PP$ (0.4 g, 0.39 mmol) in CH_2Cl_2 (50 mL) was treated with N(H)dpa (3.7 mL, 1.98 mmol), and the reaction mixture was stirred at room temperature for 24 h. Impurities in this mixture were then extracted with water (3 × 25 mL); the organic layer was dried over anhydrous Na_2SO_4 and the solvent removed under vacuum. The purple residue was crystallized from CH_2Cl_2/hexane, and the purple crystals were washed with hexane (0.32 g, 49% yield). ^{1}H NMR signals (ppm) in DMSO-d_6: 8.87 (s, 8H, βH), 8.55 (d, J = 4.1 Hz, 8H, H6/6′), 8.37 (d, J = 8.3 Hz, 8H, oH), 8.24 (d, J = 8.4 Hz, 8H, mH), 7.83 (t, 8H, H4/4′), 7.49 (d, J = 7.9 Hz, 8H, H3/3′), 7.34 (t, J = 6.2 Hz, 8H, H5/5′), 4.90 (s, 16H, CH_2), −2.96 (s, 2H, NH). ESI-MS (m/z): $[M + H]^+$ = 1660.4881, $[M + 2H]^{2+}$ = 830.7465. Calcd for $[M + H]^+$ = 1660.4886, $[M + 2H]^{2+}$ = 830.7443.

*[[Re(CO)$_3$]$_4$T(N(SO$_2$C$_6$H$_4$)dpa)P](BF$_4$)$_4$ (**6**).* [Re(CO)$_3$(CH_3CN)$_3$]-BF_4 (28 mg, 0.058 mmol) was added to a solution of T(N($SO_2C_6H_4$)-dpa)P (20 mg, 0.012 mmol) in a mixture of chloroform/acetone (25 mL/5 mL). The reaction mixture was heated at reflux for 16 h and then reduced to dryness by rotary evaporation. The maroon residue obtained was quickly washed with CH_2Cl_2, dissolved in acetone, and the resultant solution layered with hexane to give a maroon precipitate (15 mg, 40% yield). ^{1}H NMR signals (ppm) in DMSO-d_6: 9.19 (s, 8H, βH), 9.01 (d, J = 5.4 Hz, 8H, H6/6′), 8.84 (s, 16H, o and mH), 8.14 (t, J = 7.9 Hz, 8H, H4/4′), 7.71 (d, J = 8.0 Hz, 8H, H3/3′), 7.58 (t, J = 6.8 Hz, 8H, H5/5′), 5.98 (d, J = 16.4 Hz, 8H, CH_2), 4.97 (d, J = 16.4 Hz, 8H, CH_2), −2.81 (s, 2H, NH).

RESULTS AND DISCUSSION

Synthesis of N(SO_2R)dpa and [Re(CO)$_3$(N(SO_2R)dpa)]X (X = PF_6 or BF_4). Potentially tridentate ligands with R = Me, tmb, dmb, tol, and Me_2Nnap groups at the central N (Figure 1) were synthesized in good yield by coupling N(H)dpa with the relevant sulfonyl chloride. NMR spectral data indicated that the products were uncontaminated with byproducts and could be used without further purification (cf. Experimental Section and Supporting Information, Figure S1). Aqueous [Re-(CO)$_3$(H_2O)$_3$]OTf[36] was used to prepare [Re-(CO)$_3$(N(SO_2R)dpa)]X complexes **1**−**5** (Scheme 1). NMR spectra of the new complexes are illustrated below or in the Supporting Information, Figure S2. No change was observed in the ^{1}H NMR signals of **1** and **4** (5 mM, DMSO-d_6), even after 6 months.

Synthesis of the Porphyrin, T(N($SO_2C_6H_4$)dpa)P, and the 4:1 Re Adduct, [[Re(CO)$_3$]$_4$T(N($SO_2C_6H_4$)dpa)P](BF$_4$)$_4$. We have utilized our synthetic approach reported for T($R^1R^2NSO_2C_6H_4$)P [R^1 = N-py-n-CH_2 (n = 2 or 4) and R^2 = alkyl)][41] to prepare T(N($SO_2C_6H_4$)dpa)P, a porphyrin bearing four tertiary N(SO_2)dpa moieties (Scheme 2). Because the porphyrin is not soluble in water, we employed the [Re(CO)$_3$(CH_3CN)$_3$]BF_4 precursor[37] to form [[Re(CO)$_3$]$_4$T-(N($SO_2C_6H_4$)dpa)P](BF$_4$)$_4$. In this 4:1 adduct, each *fac*-[$Re^I(CO)_3]^+$ moiety is coordinated to three N-donor atoms (of a peripheral tertiary dpa moiety) linked to the porphyrin aryl group. In previous work, Alessio and co-workers utilized the [Re(CO)$_3$($DMSO$)$_3$]$^+$ precursor to synthesize [Re-(CO)$_3$(bipyridine)($DMSO$)]$^+$,[42] which was then used to prepare 1:1 and 4:1 adducts between $Re^I(CO)_3$(bipyridine)

dx.doi.org/10.1021/ic302180t | Inorg. Chem. 2013, 52, 2412−2421

Table 2. Selected Bond Distances (Å) and Angles (deg) for $[Re(CO)_3(N(SO_2Me)dpa)]PF_6$ (1) and $[Re(CO)_3(N(SO_2tmb)dpa)]PF_6$ (2), $[Re(CO)_3(N(SO_2tol)dpa)]PF_6$ (4), and $[Re(CO)_3(N(SO_2Me_2Nnap)dpa)]BF_4$ (5)

	1	2	4	5
		Bond Distances		
Re−N1	2.1736(17)	2.175(5)	2.179(3)	2.170(4)
Re−N2	2.2826(16)	2.279(5)	2.275(3)	2.272(4)
Re−N3	2.1948(18)	2.175(5)	2.173(3)	2.181(4)
Re−C1	1.928(2)	1.909(7)	1.937(4)	1.925(6)
Re−C2	1.905(2)	1.893(7)	1.907(5)	1.900(6)
Re−C3	1.936(2)	1.936(8)	1.938(5)	1.945(6)
S1−O5	1.4288(17)	1.433(5)	1.416(3)	1.425(4)
S1−O4	1.4299(15)	1.428(4)	1.437(3)	1.420(3)
S1−N2	1.7552(17)	1.755(5)	1.752(3)	1.776(4)
		Bond Angles		
N1−Re−N2	77.16(6)	76.98(18)	75.86(12)	78.08(14)
N1−Re−N3	80.12(7)	86.49(19)	78.85(12)	78.42(16)
N2−Re−N3	76.25(6)	73.96(18)	77.58(11)	76.37(15)
C2−Re−N1	94.33(8)	100.3(3)	96.83(16)	95.53(19)
C3−Re−N1	96.45(8)	90.4(2)	95.52(15)	96.96(19)
C2−Re−N3	96.55(8)	94.6(3)	97.25(17)	96.5(2)
C1−Re−N3	96.18(8)	96.1(2)	96.56(14)	97.37(19)
Re−N2−S1	111.00(8)	109.8(2)	111.68(15)	111.91(19)
Re−N2−C9	107.70(11)	109.4(3)	104.1(2)	108.3(3)
Re−N2−C10	108.47(12)	104.1(3)	110.1(2)	106.5(3)
S1−N2−C9	109.69(13)	110.9(4)	109.5(2)	109.1(3)
S1−N2−C10	108.22(12)	113.5(4)	109.8(3)	109.4(3)
C9−N2−C10	111.8(2)	108.9(5)	111.5(3)	111.5(4)

units and *meso*-tetrakis(4-pyridyl)porphyrin (TpyP(4)).[43] In these Re-porphyrin adducts, only one Re−N bond, involving a peripheral *meso*-pyridyl group, links the Re moiety to the porphyrin. The $[[Re(CO)_3]_4T(N(SO_2C_6H_4)dpa)P](BF_4)_4$ adduct prepared in this study is expected to maintain its integrity better because each Re moiety is linked by three donor atoms.

Structural Results. Crystal data and details of the structural refinement for complexes **1**, **2**, **4**, and **5** are summarized in Table 1. The Re complexes reported here exhibit a pseudo octahedral structure (Figure 2), with the three carbonyl ligands occupying one face. The remaining three coordination sites are occupied by three nitrogen atoms of the tridentate ligands. The atom numbering systems in Figure 2 are used to describe the solid-state data.

The unusual and most interesting structural features of these complexes involve the sulfonamide containing the central nitrogen (N2), which is bound to Re. First, we present information on other structural aspects, beginning with a consideration of bond lengths. In $[Re(CO)_3L]^+$ complexes with prototypical NNN donor ligands, Re−N(sp^3) bond distances (generally ∼2.23−2.29 Å)[44,45] are longer than Re−N(sp^2) bond distances (generally 2.14−2.18 Å).[37,46,47] The Re−N(sp^2) bond distances involving the pyridyl groups (N1 and N3, Figure 2) of $[Re(CO)_3(N(SO_2Me)dpa)]PF_6$ (**1**), $[Re(CO)_3(N(SO_2tmb)dpa)]PF_6$ (**2**), $[Re(CO)_3(N(SO_2tol)dpa)]PF_6$ (**4**), and $[Re(CO)_3(N(SO_2Me_2Nnap)dpa)]BF_4$ (**5**) are similar and fall within a normal range (Table 2). For the most part, the Re−N(pyridyl) bond distances are not significantly different from the values reported for $[Re(CO)_3(N(H)dpa)]Br$ (2.177(5) and 2.183(5) Å)[21] and for $[Re(CO)_3(N(CH_2CO_2Et)dpa)]Br$ (2.161(6) and 2.174(5) Å).[21] In addition, superimposing the donor N and the Re atoms in $[Re(CO)_3(N(CH_2CO_2Et)dpa)]Br$ with the corresponding atoms in **1** reveals very good overlap of the dpa moieties of both compounds (Supporting Information, Figure S3). Thus, any effect of having a tertiary sulfonamide nitrogen, rather than a traditional sp^3 nitrogen, anchoring the two chelate rings is minimal.

Consistent with a rehybridization of the sulfonamide N atom from sp^2 to sp^3, the Re−N2(sp^3) bond distance involving the central sulfonamide group is significantly longer than the Re−N1(sp^2) and Re−N3(sp^2) bond distances involving the pyridyl groups for all four compounds (Table 2). The Re−N2 bond distance (2.2826(16) Å) of $[Re(CO)_3(N(SO_2Me)dpa)]PF_6$ (**1**) (Figure 2) is comparable to that of the unquestionably sp^3-hybridized N atom (2.232(4) Å) of the central donor group of $[Re(CO)_3(N(CH_2CO_2Et)dpa)]Br$.[21] These bond distances are slightly longer than that (2.187(4) Å) of the parent complex, $[Re(CO)_3(N(H)dpa)]Br$,[21] indicating that replacing the NH proton with a larger substituent leads to bond lengthening. This result is attributable mainly to steric rather than electronic effects. Thus, these comparisons clearly indicate that the sulfonamide N is a relatively strong electron donor because the SO_2 group on N2 in **1** is more bulky than the CH_2 group on N2 in $[Re(CO)_3(N(CH_2CO_2Et)dpa)]Br$.

In $[Re(CO)_3(N(SO_2Me)dpa)]PF_6$ (**1**) (Figure 2), the angles of the sulfonamide nitrogen are close to 109.5° (Table 2), another result clearly illustrating that the hybridization of the sulfonamide nitrogen has changed from sp^2 to sp^3 upon binding to Re. Similar conclusions apply to the other structurally characterized complexes in Figure 2. However, the bond angles of $[Re(CO)_3(N(SO_2tmb)dpa)]PF_6$ (**2**, Table 2) show on average a greater deviation from values for other complexes, and this deviation appears to be clearly attributable to the stacking of the tmb rings (3.8−3.9 Å contact distances) in the crystal (Supporting Information, Figure S4). This result and features of structures in the literature (see below) suggest that

dx.doi.org/10.1021/ic302180t | Inorg. Chem. 2013, 52, 2412−2421

the angles of the sulfonamide group are quite pliable, a feature that can lead to ligands which exhibit coordinative flexibility.[27]

Fewer than 20 complexes are known in which tertiary sulfonamides have been shown to bind to metals;[26−33] in all of these reported compounds the sulfonamide N is positioned advantageously by ligand rings. The evidence for angles close to 109.5° (Table 2) clearly indicates that binding to Re^{I} results in sp^2-to-sp^3 rehybridization of the tertiary sulfonamide nitrogen. This finding that all angles are close to the tetrahedral value is a common feature in the complexes of many metals in various oxidation states (Ni^{II}, Co^{II}, Mn^{II}, Cu^{II}, La^{III})[26,27,32,33] with a bound sulfonamide. One useful approach to appreciating the sp^3 nature of the sulfonamide nitrogen is to determine the distance by which the N lies out of the plane defined by the S atom and the two C atoms attached to N. For complexes **1**, **2**, **4**, and **5**, this out-of-the-plane distance ranges from 0.486−0.515 Å. Likewise, for complexes with other metals and differing widely in the ligands and geometries, values of 0.38−0.51 Å are typically found.[26,27,32,33] In contrast, for complexes in which the sulfonamide nitrogen is not bound, the out-of-the-plane distances in reported structures typically range from 0.06−0.125 Å.[26,27]

New complexes **1**, **2**, **4**, and **5** are the only examples of complexes with a tridentate ligand having a coordinated tertiary sulfonamide with a typical M−N(sp^3) distance. In almost all cases, the metal-bound tertiary sulfonamide nitrogen and the donors of the adjacent chelate rings occupy the face of an octahedron[26,28,33] or have a similar arrangement in complexes with other geometries.[29,30] In other words, these three N-donor atoms and the metal atom typically do not define a common plane. However, because the sulfonamide group is pliable, when the R group attached to sulfur possesses a suitably positioned donor atom, the ligand can coordinate in a tripodal tetradentate fashion.[27] In fact, only in such rare cases is the M−N(sulfonamide) bond length as short as a typical M−N(sp^3) distance.[27] In these rare tripodal tetradentate cases, the sulfonamide N and the two flanking N donor atoms linked to it coordinate meridionally, not facially.[27] In the only other case of meridional coordination, the M−N(sulfonamide) bond length is long (2.298 Å).[27] A ten-coordinate square antiprismatic La^{III} complex with one macrocyclic ligand derived from cyclen, having one sulfonamide N donor and three amine N donors, has a long La^{III}−N(sulfonamide) bond, and the coordination mode is between facial and meridional.[32]

For compounds **1**, **2**, **4**, and **5**, the relatively short metal-to-nitrogen(sulfonamide) bond (adjusting for the Re^{I} characteristics) correlates with a relatively long N−S bond. The N−S distances found in this work are 1.755−1.776 Å. In the rare examples in which the M−N(sulfonamide) bond length reflects a strong bond (enforced by the tripodal nature of the ligand), the N−S distance is ∼1.73−1.76 Å.[27] For more common cases in which the M−N(sulfonamide) bond length is much longer than the typical value for the M−N distance of that metal in its oxidation state, the N−S distance is shorter, ∼1.7 Å or less.[27] For complexes in which the sulfonamide is not coordinated, the N−S distance is about 1.62−1.64 Å.[27] Thus, although the bond angles appear to reflect sp^2-to-sp^3 rehybridization of the sulfonamide nitrogen, weakly coordinated or noncoordinated sulfonamide groups have N−S bonds possessing considerable double-bond character.[27] The N−S bond length in the square antiprismatic La^{III} complex[32] is consistent with this relationship.

NMR Spectroscopy. T($N(SO_2C_6H_4)$dpa)P and all complexes and ligands reported here were characterized by NMR spectroscopy in DMSO-d_6 (NMR data and assignments are presented in the Experimental Section). In the free $N(SO_2R)$-dpa (R = Me, tmb, dmb, tol, and Me_2Nnap) ligands, the signal for the methylene groups is a singlet (Figure 3 and Supporting Information, Figure S1). The protons in each group are magnetically equivalent because the sulfonamide group can achieve a time-averaged planar geometry with both methylene groups in the pseudo plane.

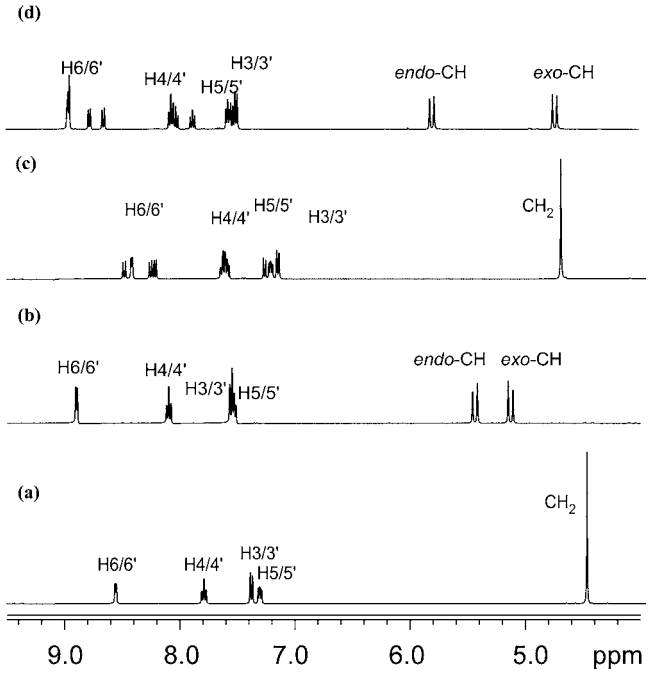

Figure 3. Comparison of the ^{1}H NMR spectra of ligands ($N(SO_2Me)$dpa (a), $N(SO_2Me_2Nnap)$dpa (c)) and the corresponding Re complexes ([$Re(CO)_3(N(SO_2Me)dpa)$]PF_6 (**1**) (b), [$Re(CO)_3(N(SO_2Me_2Nnap)dpa)$]$BF_4$ (**5**) (d)) in DMSO-d_6 at 25 °C.

The methylene groups of [$Re(CO)_3(N(SO_2R)dpa)$]X complexes **1**−**5** are related by a mirror plane. However, unlike the case of the free ligand, the two protons on each methylene group are not magnetically equivalent (cf. Figure 2); they project toward and away from the carbonyl ligands and are designated as *endo*- and *exo*-CH protons, respectively (Chart 1). The methylene protons give rise to two doublets (Figure 3 and Supporting Information, Figure S2) rather than one singlet, as found for the free ligand (Figure 3 and Supporting Information, Figure S1).

Bidentate coordination of the $N(SO_2R)$dpa ligand via the two pyridyl N atoms also prevents the tertiary sulfonamide group from achieving a time-averaged planar geometry. Methylene doublets for $N(SO_2R)$dpa ligands in the bidentate binding mode were observed for the pseudo square planar complexes, $Pd^{II}(N(SO_2tol)dpa)Cl_2$[48] and $Pt^{II}(N(SO_2R)dpa)$-Cl_2.[49] (These Pt^{II} complexes contain the $N(SO_2R)$dpa ligands used in the current study, Figure 1.) The geminal coupling constants also were similar; for example, J = 15.8 Hz for **1** and J = 15.0 Hz for $Pt(N(SO_2Me)dpa)Cl_2$. Furthermore, no trend was observed in the shifts of the methylene ^{1}H NMR signals. Thus, the methylene signals of the coordinated $N(SO_2Me)$dpa ligand are not useful for assessing binding mode (bidentate or tridentate).

The methyl ^{1}H NMR signal of [$Re(CO)_3(N(SO_2Me)dpa)$]-PF_6 (**1**) is shifted downfield by 0.76 ppm relative to the

dx.doi.org/10.1021/ic302180t | Inorg. Chem. 2013, 52, 2412−2421

Chart 1. Designation of the Methylene Group *endo*-CH and *exo*-CH Protons in Complexes 1−6

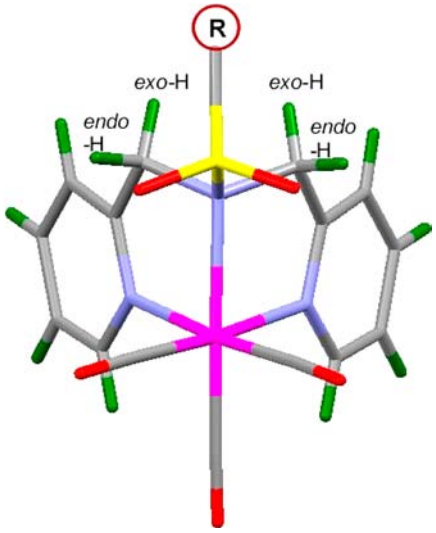

$N(SO_2Me)$dpa ligand; however, this signal shifted downfield by only 0.10 ppm for Pt($N(SO_2Me)$dpa)Cl_2.[49] The downfield shift for **1** can be explained best by the inductive effect resulting from a direct N−Re bond (Figure 2) compared to the absence of a N−Pt bond in Pt($N(SO_2Me)$dpa)Cl_2. Thus, for the $N(SO_2Me)$dpa complexes, the methyl group ^{1}H NMR shift appears to provide a good spectroscopic handle for assigning binding mode.

COSY spectra were useful in assigning the aromatic signals of the free $N(SO_2Me)$dpa ligand and [Re(CO)$_3$($N(SO_2Me)$-dpa)]PF_6 (**1**) in DMSO-d_6 (Supporting Information, Figures S5 and S6). All of the aromatic signals for **1** were shifted more downfield than the corresponding signal of the free ligand. For example, the most downfield doublet (8.50 ppm) of the free $N(SO_2Me)$dpa ligand is the pyridyl H6/6′ signal (consistent with the close proximity of the H6/6′ protons to a pyridyl nitrogen); the H6/6′ signal has an even more downfield shift (8.89 ppm) in **1**, as expected from the Re^I electron-withdrawing inductive effect on the coordinated pyridyl group. The pyridyl H6/6′ signal (9.24 ppm) of Pt($N(SO_2Me)$dpa)Cl_2 is even more downfield than that of **1**. The same trend in H6/6′ shifts is seen when comparing the spectra of [Re(CO)$_3$($N(SO_2$tmb)-dpa)]PF_6 (**2**) and Pt($N(SO_2$tmb)dpa)Cl_2. We attribute the greater downfield shifts in the Pt complexes to a greater electron-withdrawing inductive effect of Pt^{II} as compared to Re^I. In DMSO-d_6 for L = 3-(4′-methylpyridin-2′-yl)-5,6-dimethyl-1,2,4-triazine,[50] the pyridyl H6 signal appeared more downfield for $PtLCl_2$ (9.35 ppm)[50] than for [Re(CO)$_3$L-(CH_3CN)]BF_4 (8.97 ppm),[49] a result indicating that Pt^{II} does indeed have a generally greater inductive effect than Re^I. This greater effect for Pt^{II} than for Re^I adds further confidence to our analysis that the small downfield shift for the Me ^{1}H NMR signal for Pt($N(SO_2Me)$dpa)Cl_2 compared to that for **1** indicates that the sulfonamide N binds to Re^I but not to Pt^{II}; otherwise, the Me ^{1}H NMR signal for the Pt^{II} compound would be more downfield than that for the Re^I compound.

For [Re(CO)$_3$($N(SO_2Me)$dpa)]PF_6 (**1**), we could not use the weak NOE cross-peaks from the methyl signal to both methylene doublets to assign unambiguously the doublets to *exo*-CH and *endo*-CH protons (Chart 1). However, the NOE cross-peak from the pyridyl H3/3′ signal (7.57 ppm) was larger to the methylene doublet at 5.13 ppm than to the doublet at 5.44 ppm (not shown). In the molecular structure of **1**, nonbonded distances of ∼2.44 and 2.45 Å between the pyridyl H3/3′ and the *exo*-CH protons are shorter than the nonbonded distances of 3.02 and 3.09 Å between H3/3′ and the *endo*-CH protons. This information, combined with the size of the NOE cross-peaks, indicates that the more upfield signal (5.13 ppm) is the *exo*-CH doublet for **1**.

Except for the distorted [Re(CO)$_3$($N(SO_2$tmb)dpa)]PF_6 (**2**) complex, all of the nonbonded distances from the pyridyl H3/3′ protons of structurally characterized complexes are shorter to the *exo*-CH protons (∼2.5 Å) than to the *endo*-CH protons (∼3.0 Å). In a ROESY spectrum of [Re(CO)$_3$($N(SO_2$dmb)-dpa)]PF_6 (**3**) in DMSO-d_6 (Supporting Information, Figure S7), an NOE cross-peak from the CH doublet at 4.55 ppm to the H3/3′ signal assigns this doublet to the *exo*-CH protons. An NOE cross-peak between the dmb H2/6 signal (7.96 ppm) and the CH doublet at 5.25 ppm assigns this doublet to the *endo*-CH signal. Thus, the *exo*-CH and *endo*-CH assignments are mutually confirmed because the nonbonded distances from the H2/6 protons in [Re(CO)$_3$($N(SO_2$tol)dpa)]PF_6 (**4**) to the *exo*-CH and *endo*-CH protons are 3.06 and 2.59 Å, respectively.

Changes in the NMR signals in DMSO-d_6 for T-($N(SO_2C_6H_4)$dpa)P on formation of [[Re(CO)$_3$]$_4$T-($N(SO_2C_6H_4)$dpa)P]$(BF_4)_4$ (**6**) (Figure 4) establish beyond

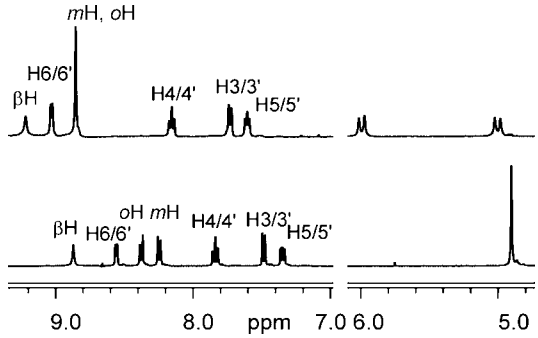

Figure 4. Comparison of ^{1}H NMR spectra of T($N(SO_2C_6H_4)$dpa)P (*bottom*) and [[Re(CO)$_3$]$_4$T($N(SO_2C_6H_4)$dpa)P]$(BF_4)_4$ (**6**) (*top*) in DMSO-d_6 at 25 °C.

question that the formulation of **6** is correct. The methylene group singlet for T($N(SO_2C_6H_4)$dpa)P becomes two doublets in **6**. In the ROESY spectrum in DMSO-d_6 (not shown), an NOE cross-peak from the doublet at 4.97 ppm to the pyridyl H3/3′ signal assigns that doublet to the *exo*-CH protons, and the NOE cross-peak from the other methylene doublet (5.97 ppm) to the phenylene signal (8.84 ppm) assigns this doublet to the *endo*-CH protons (Chart 1).

Coordination of the four Re moieties to T($N(SO_2C_6H_4)$dpa)P leads to the apparent singlet signal (8.84 ppm, Figure 4) for the clearly inequivalent phenylene *ortho* and *meta* protons of **6** (Scheme 2). We attribute this interesting spectral feature to a similar chemical shift of the signals of the phenylene group, leading to non-first-order spectral features in this aromatic region. Binding of the porphyrin sulfonamide groups to Re leads to a larger downfield shift change (by 0.60 ppm) of the *m*-H (H2/6) signal (for the phenylene protons closest to Re) versus the smaller downfield shift change (by 0.37 ppm) of the phenylene *o*-H (H3/5) signal. This result fully supports the proposed structure.

dx.doi.org/10.1021/ic302180t | *Inorg. Chem.* 2013, 52, 2412−2421

The ^{1}H NMR spectrum of [[Re(CO)$_3$]$_4$T(N(SO$_2$C$_6$H$_4$)-dpa)P](BF$_4$)$_4$ (**6**) in DMSO-d_6 (Figure 4) reveals other effects of Re coordination to the pyridyl nitrogen. The ^{1}H NMR signal for the pyrrole βH (Scheme 2) is ~0.3 ppm more downfield than the βH signal of the free T(N(SO$_2$C$_6$H$_4$)dpa)P ligand. The pyridyl H6/6′ signal (J = 5.4 Hz) of **6** appears at 9.01 ppm versus 8.55 ppm for T(N(SO$_2$C$_6$H$_4$)dpa)P. The ^{1}H NMR shifts of the pyridyl signals of **6** are very similar to those of the crystallographically characterized complex **1**, another indication of the presence of a Re−N(pyridyl) bond. Furthermore, the two methylene doublets for **6** have J = 16.4 Hz, a value very similar to that for **1** (J = 15.8 Hz). As is true for the smaller complexes, the two doublets for [[Re(CO)$_3$]$_4$T(N(SO$_2$C$_6$H$_4$)-dpa)P](BF$_4$)$_4$ can be attributed to the fact that the CH$_2$−N(SO$_2$R)−CH$_2$ grouping cannot achieve the time-averaged planarity required for magnetic equivalence.

In general, the relatively downfield and upfield methylene doublets are assigned to the *endo*-CH and the *exo*-CH signals, respectively, for complexes **1**−**6**. However, there is some variability in the exact shift values (cf. Experimental Section, Supporting Information). The shift dependence on the nature of R is complicated, but we can explain the shift dependence within the series of R groups that have methyl-substituted benzene rings (tol, dmb, and tmb). The *exo*-CH signals all have nearly identical shifts (Supporting Information, Figure S2) and the *endo*-CH signals for tol and dmb also have nearly identical shifts. However, the *endo*-CH signal for the tmb complex is relatively upfield. The two ortho methyl groups of tmb appear to position the ring so that it has an anisotropic shielding of the *endo*-CH proton. This positioning is found in the molecular structure and may be the reason for the stacking interactions found in the solid (Supporting Information, Figures S4 and S8).

Effects of Bases. As mentioned above, these complexes are stable for long periods in DMSO-d_6. However, when basic ligands were added to a 5 mM solution of [Re(CO)$_3$(N(SO$_2$Me)dpa)]PF$_6$ in acetonitrile-d_3 (4-dimethylaminopyridine, 4-methylimidazole, or 3,5-lutidine) or in DMSO-d_6 (4-dimethylaminopyridine), complicated ^{1}H NMR spectral changes attributable to a decomposition reaction were observed. For 4-dimethylaminopyridine, decomposition was observed in the first spectrum (recorded after 15 min); however, for 3,5-lutidine, decomposition was first noticeable in a spectrum recorded after 24 h. When triethylamine (a strong base but a very poor ligand) was added to a similar 5 mM solution of [Re(CO)$_3$(N(SO$_2$Me)dpa)]PF$_6$, immediate decomposition was observed. All spectra contained a very similar set of peaks attributable to decomposition products. These results are consistent with base-catalyzed decomposition of the coordinated N(SO$_2$Me)dpa ligand. In contrast, adding 1 molar equiv of triethylamine to a 5 mM acetonitrile-d_3 solution of the N(SO$_2$Me)dpa ligand itself produced no changes in the ^{1}H NMR spectrum, even after 2 weeks. These observations suggest that the ligand decomposition is promoted by the electron-withdrawing inductive effect of the Re$^{\mathrm{I}}$(CO)$_3$ metal center.

The absence of any need to protect the two terminal pyridyl donor nitrogens is an advantage of using the dpa framework for bioconjugation; however, the electron-withdrawing pyridyl group may contribute to the base-catalyzed decompostion. We have thus redesigned the ligand framework for future studies.

Summary and Conclusions. The [Re(CO)$_3$(N(SO$_2$R)-dpa)]X (X = PF$_6$ or BF$_4$) complexes synthesized and characterized as a prelude to radiopharmaceutical studies with novel N(SO$_2$R)dpa ligands provide structural evidence establishing that the Re−N bond formed between a tertiary sulfonamide N and Re can have a normal length. Because there are distinctive NMR spectral features associated with such binding in the N(SO$_2$R)dpa ligands, it is clear that the tertiary sulfonamide N binds to Re even in cases such as [Re(CO)$_3$(N(SO$_2$dmb)dpa)]PF$_6$ (**3**), for which an X-ray structure could not be obtained.

Monodentate tertiary sulfonamides do not bind metals. Thus, as illustrated in the examples here and in previous reports,[28−31] tertiary sulfonamides bind metals via the N atom only when geometrical restraints are enforced by the ligand so as to place the N atom in a favorable position to form a bond. The tertiary sulfonamide nitrogen adopts stereochemical and structural features consistent with sp^3 hybridization. As a result, the N atom accommodates a facial tridentate geometry when the sulfonamide anchors two chelate rings. Of note, sulfonamide binding in the [Re$^{\mathrm{I}}$(CO)$_3$L]$^+$ complexes described in this study is facilitated by sp^2-to-sp^3 rehybridization of the sulfonamide nitrogen. In such complexes, the tertiary sulfonamide appears to be a relatively good donor, as judged by the near-normal Re−N bond length and the relatively long N−S bond. In most cases reported in the literature, the M−N bond is long, and the N−S bond is relatively short.[26,27,32]

The conjugation approach described here has potentially wide applications. This prospect is supported by our results showing that a sulfonamide can be used to conjugate the *fac*-[Re$^{\mathrm{I}}$(CO)$_3$]$^+$ core unit to a dansyl group or a porphyrin. We anticipate no limitation in conjugating other molecules to such a core or in extending this chemistry to ^{99m}Tc analogues. Our results demonstrate that the tertiary sulfonamide linkage may be utilized for tethering biologically important molecules, and we are confident that the chemistry with the *fac*-[Re$^{\mathrm{I}}$(CO)$_3$]$^+$ core reported here can be readily extended to the *fac*-[^{99m}Tc$^{\mathrm{I}}$(CO)$_3$]$^+$ core.

■ ASSOCIATED CONTENT

Supporting Information

Crystallographic data for [Re(CO)$_3$(N(SO$_2$Me)dpa)]PF$_6$ (**1**), [Re(CO)$_3$(N(SO$_2$tmb)dpa)]PF$_6$ (**2**), [Re(CO)$_3$(N(SO$_2$tol)-dpa)]PF$_6$ (**4**), and [Re(CO)$_3$(N(SO$_2$Me$_2$Nnap)dpa)]BF$_4$ (**5**) in CIF format; ^{1}H NMR spectra in DMSO-d_6 of complexes **1** to **5** and of the N(SO$_2$R)dpa ligands used to form these complexes; figure illustrating the overlay of Re, N1, N2 and N3 atoms of **1** and [Re(CO)$_3$(N(CH$_2$CO$_2$Et)dpa)]Br; figure depicting stacking of tmb rings in **2**; COSY spectra of N(SO$_2$Me)dpa and **1**; ROESY spectrum of [Re(CO)$_3$(N(SO$_2$dmb)dpa)]BF$_4$ (**3**) in DMSO-d_6; and an informative side view of [Re(CO)$_3$(N(SO$_2$tmb)dpa)]PF$_6$ (**2**). This material is available free of charge via the Internet at http://pubs.acs.org.

■ AUTHOR INFORMATION

Corresponding Author

*E-mail: lmarzil@lsu.edu.

Notes

The authors declare no competing financial interest.

■ ACKNOWLEDGMENTS

This work was supported in part by the National Institutes of Health (R37 DK038842-22). Purchase of the diffractometer was made possible by Grant LEQSF (1999-2000)-ENH-TR-13, administered by the Louisiana Board of Regents. L.G.M. thanks the RAYMOND F. SCHINAZI INTERNATIONAL EXCHANGE PROGRAMME between the University of Bath, U.K., and Emory University, Atlanta, GA, U.S.A., for a Faculty Fellowship.

■ REFERENCES

(1) Schibli, R.; Schubiger, A. P. *Eur. J. Nucl. Med. Mol. Imaging* **2002**, *29*, 1529−1542.
(2) Liu, S. *Chem. Soc. Rev.* **2004**, *33*, 445−461.
(3) Lipowska, M.; Marzilli, L. G.; Taylor, A. T. *J. Nucl. Med.* **2009**, *50*, 454−460.
(4) Lipowska, M.; He, H.; Malveaux, E.; Xu, X.; Marzilli, L. G.; Taylor, A. T. *J. Nucl. Med.* **2006**, *47*, 1032−1040.
(5) Maresca, K. P.; Marquis, J. C.; Hillier, S. M.; Lu, G.; Femia, F. J.; Zimmerman, C. N.; Eckelman, W. C.; Joyal, J. L.; Babich, J. *Bioconjugate Chem.* **2010**, *21*, 1032−1042.
(6) Alberto, R.; N'Dongo, H. P.; Clericuzio, M.; Bonetti, S.; Gabano, E.; Cassino, C.; Ravera, M.; Osella, D. *Inorg. Chim. Acta* **2009**, *362*, 4785−4790.
(7) Alberto, R.; Schibli, R.; Egli, A.; Schubiger, A. P.; Abram, U.; Kaden, T. A. *J. Am. Chem. Soc.* **1998**, *120*, 7987−7988.
(8) Alberto, R.; Ortner, K.; Wheatley, N.; Schibli, R.; Schubiger, A. P. *J. Am. Chem. Soc.* **2001**, *123*, 3135−3136.
(9) Schibli, R.; Bella, R. L.; Alberto, R.; Garcia-Garayoa, E.; Ortner, K.; Abram, U.; Schubiger, A. P. *Bioconjugate Chem.* **2000**, *11*, 345−351.
(10) Bartholomä, M.; Valliant, J.; Maresca, K. P.; Babich, J.; Zubieta, J. *Chem. Commun. (Cambridge, U.K.)* **2009**, 493−512.
(11) Taylor, A. T.; Lipowska, M.; Marzilli, L. G. *J. Nucl. Med.* **2010**, *51*, 391−396.
(12) Taylor, A.; Lipowska, M.; Verdes, L.; Cai, H.; Folks, R.; Malveaux, E. *J. Nucl. Med.* **2012**, *53* (Supplement 1), 180.
(13) Desbouis, D.; Struthers, H.; Spiwok, V.; Küster, T.; Schibli, R. *J. Med. Chem.* **2008**, *51*, 6689−6698.
(14) Abram, U.; Alberto, R. *J. Braz. Chem. Soc.* **2006**, *17*, 1486−1500.
(15) Alberto, R.; Schibli, R.; Schubiger, A. P.; Abram, U.; Pietzsch, H. J.; Johannsen, B. *J. Am. Chem. Soc.* **1999**, *121*, 6076−6077.
(16) He, H.; Lipowska, M.; Xu, X.; Taylor, A. T.; Marzilli, L. G. *Inorg. Chem.* **2007**, *46*, 3385−3394.
(17) He, H. Y.; Lipowska, M.; Christoforou, A. M.; Marzilli, L. G.; Taylor, A. T. *Nucl. Med. Biol.* **2007**, *34*, 709−716.
(18) Kyprianidou, P.; Tsoukalas, C.; Chiotellis, A.; Papagiannopolu, D.; Raptopolou, C. P.; Terzis, A.; Pelecanou, M.; Papadopoulos, M.; Pirmettis, I. *Inorg. Chim. Acta* **2011**, *370*, 236−242.
(19) Boros, E.; Häfeli, U. O.; Patrick, B. O.; Adam, M. J.; Orvig, C. *Bioconjugate Chem.* **2009**, *20*, 1002−1009.
(20) Klenc, J.; Lipowska, M.; Marzilli, L. G.; Taylor, A. T. *Eur. J. Inorg. Chem.* **2012**, 4334−4344.
(21) Banerjee, S. R.; Levadala, M. K.; Lazarova, N.; Wei, L.; Valliant, J. F.; Stephenson, K. A.; Babich, J. W.; Maresca, K. P.; Zubieta, J. *Inorg. Chem.* **2002**, *41*, 6417−6425.
(22) Storr, T.; Fisher, C. L.; Mikata, Y.; Yano, S.; Adam, M. J.; Orvig, C. *Dalton Trans.* **2005**, 654−655.
(23) Xia, J.; Wang, Y.; Li, G.; Yu, J.; Yin, D. *J. Radioanal. Nucl. Chem.* **2009**, *279*, 245−252.
(24) White, D. J.; Kuppers, H. J.; Edwards, A. J.; Watkin, D. J.; Cooper, S. R. *Inorg. Chem.* **1992**, *31*, 5351−5352.
(25) Schibli, R.; Alberto, R.; Abram, U.; Abram, S.; Egli, A.; Schubiger, A. P.; Kaden, T. A. *Inorg. Chem.* **1998**, *37*, 3509−3316.
(26) Lee, W.; Tseng, H.; Kuo, T. *Dalton Trans.* **2007**, 2563−2570.
(27) Veltzé, S.; Egdal, R. K.; Johansson, F. B.; Bond, A. D.; McKenzie, C. J. *Dalton Trans.* **2009**, 10495−10504.
(28) Klingele, M. H.; Moubaraki, B.; Murray, K. S.; Brooker, S. *Chem.—Eur. J.* **2005**, *11*, 6962−6973.
(29) Caselli, A.; Cesana, F.; Gallo, E.; Casati, N.; Macchi, P.; Sisti, M.; Celentano, G.; Cenini, S. *Dalton Trans.* **2008**, 4202−4205.
(30) Calligaris, M.; Carugo, O.; Crippa, G.; De Santis, G.; Di Casa, M.; Fabbrizzi, L.; Poggi, A.; Seghi, B. *Inorg. Chem.* **1990**, *29*, 2964−2970.
(31) Sun, C.-H.; Chow, T. J.; Liu, L.-K. *Organometallics* **1990**, *9*, 560−565.
(32) Gunnlaugsson, T.; Leonard, J.; Mulready, S.; Nieuwenhuyzen, M. *Tetrahedron* **2004**, *60*, 105−113.
(33) Seidler-Egdal, R. K.; Johannson, F. B.; Veltzé, S.; Skou, E. M.; Bond, A. D.; McKenzie, C. J. *Dalton Trans.* **2011**, *40*, 3336−3345.
(34) Toscano, P. J.; Jordan, K. F.; Engelhardt, L. M.; Skelton, B. W.; White, A. H.; Marzilli, P. A. *Polyhedron* **1990**, *9*, 1079−1085.
(35) Toscano, P. J.; Marzilli, L. G. *Inorg. Chem.* **1983**, *22*, 3342−3350.
(36) He, H.; Lipowska, M.; Xu, X.; Taylor, A. T.; Carlone, M.; Marzilli, L. G. *Inorg. Chem.* **2005**, *44*, 5437−5446.
(37) Perera, T.; Abhayawardhana, P.; Fronczek, F. R.; Marzilli, P. A.; Marzilli, L. G. *Eur. J. Inorg. Chem.* **2012**, 618−627.
(38) Gonsalves, A. M. R.; Johnstone, R. A. W.; Pereira, M. M.; de SantAna, A. M. P.; Serra, A. C.; Sobral, A. J. F. N.; Stocks, P. A. *Heterocycles* **1996**, *43*, 829−838.
(39) Otwinowski, Z.; Minor, W. *Macromolecular Crystallography, Part A, Methods in Enzymology*; Academic Press: New York, 1997; Vol. *276*, pp 307−326.
(40) Sheldrick, G. M. *SHELXL97, Program for Crystal Structure Solution and Refinement*; University of Göttingen: Göttingen, Germany, 1997.
(41) Manono, J.; Marzilli, P. A.; Fronczek, F. R.; Marzilli, L. G. *Inorg. Chem.* **2009**, *48*, 5626−5635.
(42) Casanova, M.; Zangrando, E.; Munini, F.; Iengo, E.; Alessio, E. *Dalton Trans.* **2006**, 5033−5045.
(43) Ghirotti, M.; Chioboli, C.; Indelli, M. T.; Scandola, F.; Casanova, M.; Iengo, E.; Alessio, E. *Inorg. Chim. Acta* **2007**, *360*, 1121−1130.
(44) Christoforou, A. M.; Marzilli, P. A.; Fronczek, F. R.; Marzilli, L. G. *Inorg. Chem.* **2007**, *46*, 11173−11182.
(45) Perera, T.; Marzilli, P. A.; Fronczek, F. R.; Marzilli, L. G. *Inorg. Chem.* **2010**, *49*, 5560−5572.
(46) Perera, T.; Fronczek, F. R.; Marzilli, P. A.; Marzilli, L. G. *Inorg. Chem.* **2010**, *49*, 7035−7045.
(47) Christoforou, A. M.; Fronczek, F. R.; Marzilli, P. A.; Marzilli, L. G. *Inorg. Chem.* **2007**, *46*, 6942−6949.
(48) Canovese, L.; Visentin, F.; Chessa, G.; Uguagliati, P.; Levi, C.; Dolmella, A.; Bandoli, G. *Organometallics* **2006**, *25*, 5355−5365.
(49) Perera, T. Chemistry of Rhenium(I) Tricarbonyl Complexes of Biomedical Relevance. Ph.D. Dissertation, Louisiana State University, Baton Rouge, LA, August 2010.
(50) Maheshwari, V.; Bhattacharyya, D.; Fronczek, F. R.; Marzilli, P. A.; Marzilli, L. G. *Inorg. Chem.* **2006**, *45*, 7182−7190.